Eur. Phys. J. D (2023)77:188
https://doi.org/10.1140/epjd/s10053-023-00768-5

THE EUROPEAN PHYSICAL JOURNAL D

Regular Article – Optical Phenomena and Photonics

Design and simulation of phase shifter based on multimode interference in photonic crystal waveguide

Haraprasad Mondal[1,a], Nistha Dutta[1,b], Mukunda Madhav Das[1,c], Swarna Bhattacharjee[1,d], Kamanashis Goswami[2,e], Somenath Dutta[3,f], Mrinal Sen[3,g]

[1] Dibrugarh University Institute of Engineering and Technology, Dibrugarh University, Assam, India
[2] Haldia Institute of Technology, Haldia, Purba Medinipur, West Bengal 721657, India
[3] Electronics Engineering, Indian Institute of Technology (ISM) Dhanbad, Jharkhand 826004, India

Received 7 June 2023 / Accepted 9 October 2023

Abstract. This paper proposes a new design for a π-phase shifter and two π/2-phase shifters, which are based on a two-dimensional rods-in-air photonic crystal waveguide. The proposed devices have been designed using both triangular and square lattice photonic crystal structures. Notably, these phase shifters do not require any external energy source to operate. To calculate the band diagram of the PhC, the plane wave expansion method was utilized, while finite-difference time-domain simulation methodology was used to estimate and examine the performance of the proposed phase shifters. The simulation results demonstrate that the proposed π-phase shifter can achieve a bandwidth of 1.5THz, whereas the π/2-phase shifters, designed on triangular and square lattice can achieve bandwidths of 1.9THz and 1.35THz, respectively. Due to their straightforward design structure and energy independence, these devices are well-suited for future generations of all-optical photonic integrated circuits.

1 Introduction

Photonics [1, 2], as a rapidly evolving technology, has gained significant attention due to its potential to overcome the limitations of existing electronic technology in meeting the increasing demand for faster data transfer and computing. Photonics has been incorporated into various fields of engineering, including communication [3], automobile [4], biomedical [5], and aeronautical [6], and is considered highly effective with enormous potential in designing high-speed computational and data processing devices and components [6–10]. Till date, several photonic devices [11–15] have seen to be developed with the implementation of various optical principles. One of the most promising photonic technologies is photonic crystals (PhCs) [16, 17], which refer to the periodic variation of the refractive index in one, two, or three dimensions. PhCs possess valuable properties such as photonic bandgap (PBG), tunable photonic bandgaps, and the ability to control optical wavelengths through bandgap mapping. PBG is a range of frequencies where light is unable to propagate through the crystal. However, by introducing defects into the crystal through modification or removal of rods or holes, light can be propagated in the PBG range, allowing for the creation of various photonic devices. In recent decades, there has been extensive research on the utilization of two-dimensional photonic crystals (2D-PhCs) for designing a wide range of devices, such as adders [18–20], subtractors [21], de-multiplexers/multiplexers [22–25], comparators [26], beam splitters [27, 28], decoders [29–33], and logic gates [34–38]. These devices leverage the unique properties of PhCs to manipulate and control light, offering potential solutions for high-speed data processing and computation. Overall, the growing demand for faster data transfer and computing is driving innovative developments in different aspects of photonics, including the generation, detection, transmission, and manipulation of optical signals. PhCs, in particular, hold great promise as a photonic technology for integrated circuits and have been extensively studied for various applications in high-speed computational and data processing devices.

Among all the devices reported till date, phase shifters are indeed crucial components in many photonics applications, including optical fiber communication systems and sensing systems. They play a vital role in

[a] e-mail: mandal.haraprasad@gmail.com
[b] e-mail: nisthadutta7@gmail.com
[c] e-mail: mukundadas03@gmail.com
[d] e-mail: swarnabhatt12@gmail.com
[e] e-mail: kamanashis.goswami@gmail.com
[f] e-mail: somenath_ece@yahoo.co.in
[g] e-mail: mrinal.sen.ahm@gmail.com (corresponding author)

Published online: 28 October 2023

manipulating light waves to achieve desired functionalities in these systems. As mentioned, phase shifting is the process of changing the phase of light, which can result in constructive or destructive interference of signals. Phase shifters are devices that enable this manipulation of the phase of light as it passes through them. Some devices, like the XOR gate, use an indirect phase shifter that relies on asymmetrical waveguides. However, this method has limitations, such as a limited tuning range, which means that it can only operate over a specific range of phase shifts. This can restrict the flexibility and versatility of the phase shifter in certain applications. Efforts are ongoing in research and development to address these limitations and improve the performance of phase shifters. Techniques such as using different materials, designs, and fabrication methods are being explored to achieve wider tuning ranges, linear responses, and improved overall performance of phase shifters in various photonics applications. Despite these limitations, phase shifters remain essential components in many optical systems, enabling a wide range of functionalities such as modulation, switching, and sensing, and continuing research in this area is driving advancements in photonics technology.

In this context, few reported literatures on optical phase shifters have been reviewed. For example, Malik et.al. [39] have reported the development and improvement of Germanium-on-silicon thermo-optic phase shifters in the 5 μm wavelength range. An efficient phase shifter achieved a tuning power of 105 mW for a 2π phase shift, which was further reduced to 16 mW for a free-standing phase shifter. To reach a power requirement of 80 mW, complete undercut using focused ion beam was employed during fabrication. Moreover Zhu. et. al. [40] have projected the fabrication of an AlN (Aluminum nitride) electro-optic phase shifter on Silicon using complementary metal–oxide–semiconductor technology. The Pockels coefficient of the deposited AlN is estimated to be approximately 1.0 pm/V for both TE and TM modes. For the TE mode, the modulation efficiency is around 240 Vcm, and for the TM mode, it is around 320 Vcm. In addition to the above phase shifters an optical phase shifter using a low-loss optical phase change material (O-PCM) called Ge2Sb2Se4Te1 (GSST) at 1.55 μm wavelength has been reported by Dhingra.et al. [41]. The design utilizes coupling between a primary SiN strip waveguide and an O-PCM-formed waveguide in its amorphous state. The primary drawback of existing phase-shifters is their dependence on external energy (electric field/heat) for operation. Moreover, their complex design hinders practical implementation in future photonic integrated circuits (PICs). To overcome these limitations, the authors designed an optical phase shifter in the linear optical domain, allowing the signal to alter its phase without the need for external energy.

In this work, the authors have proposed two different types of phase shifters, namely π-phase shifter and π/2-phase shifter, utilizing two-dimensional Photonic Crystal (2D-PhC) rods-in-air structures. One of the unique features of these proposed phase shifters is that they do not require any external energy source to function as phase shifter. The authors have designed the phase shifters by creating a defect in an array of 2D-PhC structure, where the rods are removed in the Γ-X direction to form an optical waveguide. Furthermore, a few more rods within the waveguide are removed and the diameter and position of some rods are optimized to create a circular/elliptical-shaped cavity that functions as the phase shifter. The simple design structure and the absence of any external energy requirements make these proposed devices suitable for future generations of all-optical photonic integrated circuits (PICs). The use of 2D-PhC rods-in-air structures and the optimization of rod parameters demonstrate the potential for these phase shifters to be integrated into practical photonic devices for various applications in photonics and optical communication systems.

The rest of the paper is structured into five main sections, each of which focuses on a specific aspect of the proposed phase shifter. The second section provides a detailed analysis of the photonic crystal structure and its band characteristics. This section likely explains the design of the photonic crystal and the specific characteristics of its band structure, which are important for understanding how the proposed phase shifter works. The third section provides a detailed description of the proposed π-phase shifter, including its architecture and how it works. This section also includes information about how the phase shifter has been characterized. This same section also includes a calculation of the phase shifter's bandwidth, which is an important metric for understanding its potential applications. The fourth section focuses on the architecture of the proposed π/2-phase shifter in both triangular and square lattices. This section describes how these phase shifters differ from the π-phase shifter and how they work. Similar to the previous section, this section may also include validation and bandwidth analysis of the proposed phase shifters. Finally, the section five includes the conclusion of the work. This section is typically used to summarize the main findings of the study and provide insights into the significance and potential impact of the research.

2 PhC structures and band analysis

Photonic crystals are structures that have a periodic variation of refractive index, which allows them to manipulate the propagation of light in a variety of ways. These structures can be one-dimensional (1D), two-dimensional (2D), or three-dimensional (3D) depending on the level of periodicity. This design consists of a regular array of silicon rods that are suspended in air, with a periodicity in the x and z directions. The rods are constructed with three layers for achieving symmetrical structure in the 'Y' direction. The top and bottom layers are made of silica (SiO_2), while the middle layer, which acts as the propagation layer, is made of silicon

(Si with a refractive index of 3.476). Additionally, a supporting substrate made of silicon dioxide (SiO_2) with a thickness of 1 μm is used for mechanical stability. The height of each rod is chosen to be 1 μm. Two different PhC structures have been taken to design phase shifters. First PhC structure is composed of a lattice of rods (radius of 121 nm) that are suspended in air and arranged in a triangular pattern. The lattice constant is chosen as 604 nm. Similarly, in the second PhC structure rods are arranged in square lattice and has been optimized by selecting the parameters, including a refractive index of 3.476, a lattice constant of 540 nm, and a rod radius of 120 nm.

The band diagram of the non-defect Photonic Crystal (PhC) structure (triangular lattice) has been computed by using the plane wave expansion (PWE) algorithm. Upon analyzing Fig. 1a, it is observed that the photonic band gap (PBG) exists entirely in the transverse magnetic (TM) mode with a range of normalized frequency (a/λ) equal to 0.275–0.45. This corresponds to a specific range of wavelengths, i.e., from 1342 to 2190 nm. It is intriguing to note that that the third optical window, which is defined by the International Telecommunication Union (ITU) as centered at a wavelength of 1550 nm, falls within the aforementioned normalized frequency range. This calculation confirms that the proposed device, which is based on triangular lattice structure, operates most efficiently in the TM mode and does not exhibit a band gap in the transverse electric (TE) mode. Furthermore, a W1 line defect has been created in the Z-direction (Γ-X) of the crystal, which acts as a waveguide. To examine the frequency states within the waveguide, a projected band diagram test has been performed using the PWE algorithm, as shown in Fig. 1b. It can be observed from Fig. 1b that no frequency states exist within the waveguide (in the Z-direction of the crystal) in the range of 0.275 to 0.34. However, a clearly observable projected band ranging from 0.34 to 0.44 indicates that waves can propagate through it in the above-mentioned frequency range.

In the case of a square lattice structure (square lattice) and with the application of the PWE algorithm, it is observed in Fig. 1c that a complete photonic band gap (PBG) is found in transverse magnetic (TM) mode, with a range of normalized frequency (a/λ) equal to 0.26–0.4, which corresponds to a wavelength range from 1350 to 2000 nm. A band gap has not been achieved in transverse electric (TE) mode. The third optical window, which has a wavelength of 1550 nm, is observed to lie within the normalized frequency range. Therefore, the proposed device, which is designed using a 2D-PhC square lattice structure, is observed to work perfectly in TM mode. Furthermore, a W1 line defect has been created in the Z-direction (Γ-X) of the crystal, which acts as a waveguide. To examine the frequency states within the waveguide, a projected band diagram test has been performed using the PWE algorithm, as shown in Fig. 1d. It can be observed from Fig. 1d that no frequency states exist within the waveguide (in the Z-direction of the crystal) in the range of 0.26 to 0.29. However, a clearly observable projected band ranging from 0.29 to 0.4 indicates that waves can propagate through it in the aforementioned frequency range. Based on the observations made using the PWE algorithm being applied to a square lattice structure, it has been noted that the proposed device functions perfectly in the TM mode. It should be noted that no such band gap has been identified in the transverse electric (TE) mode. In addition, these findings are significant as they suggest that the proposed device is well-suited for applications that require a complete PBG in the TM mode.

3 Π-Phase shifter

The architecture of the proposed MMI π-phase shifter is shown in Fig. 2 and is designed using a 2D photonic crystal slab. The photonic crystal is constructed using rods in air arranged in a hexagonal pattern with a lattice constant of 604 nm and rod radius of 121 nm. The device is composed of an array of 25*15 silicon rods, and the refractive index of the silicon rods is chosen as 3.476. The proposed phase shifter consists of one input port (INPUT-B) for applying a desired optical signal and one output port (OUTPUT-B). Two parallel waveguides, WAVEGUIDE-1 and WAVEGUIDE-2, have been created using a line defect by removing rods in the Γ-X direction of the PhC slab for the purpose of parallel propagation of two identical input signals. To create a π-phase shifter within the WAVEGUIDE-2, a W3 waveguide has been formed at a certain portion of the waveguide with a length of 3-period by removing two additional rows of rods in the Γ-X direction. Furthermore, at the corner portion of the W3 waveguide, rods designated as A, B, C, and D have been shifted towards the Γ-M direction (away from the center of the waveguide) by a distance of half of period, as shown in Fig. 2a.

To investigate the functionality of the proposed device, two identical continuous optical signals have been applied at the input ports of both waveguides, and applying finite difference time domain (FDTD) algorithm the electric field propagation profile of the two parallel waveguides has been obtained which is shown in Fig. 2b. Moreover, to execute the FDTD simulation process the parameters like time step, grid spacing, and boundary conditions have been taken as 0.0466 fs, Dx = 40 nm Dy = 20 nm Dz = 35 nm and boundary condition = PML (perfectly matched layer) respectively. It can be observed from Fig. 2b that the electric field propagation profiles of both waveguides are identical from the input ports to the starting portion of the π-phase shifter. As soon as the optical wave (single mode) enters the π-phase shifter, it splits into multiple modes. Subsequently, all the modes recombine with each other, forming a single mode optical wave with a phase change of π when it emits from the π-phase shifter. It has also been observed from the Fig. 2b that there is a mismatch in the electric field propagation profile at the trail portion of both waveguides, which indicated a change in the

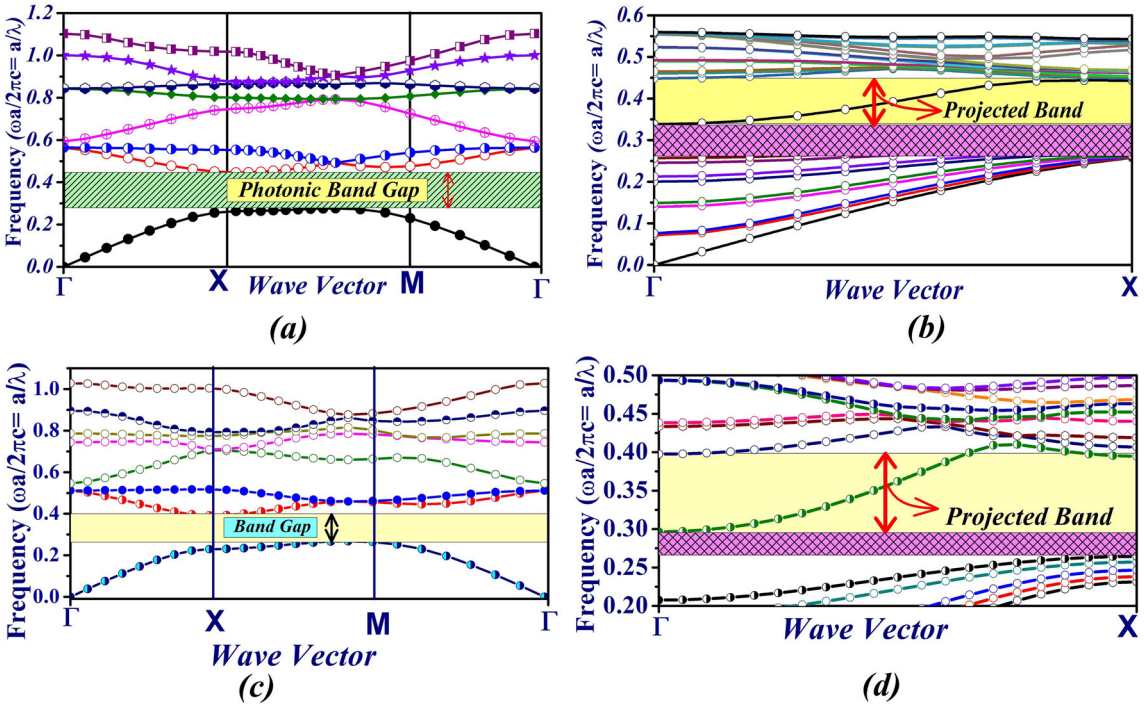

Fig. 1 (**a**) Band diagram analysis of Triangular lattice (**b**) Projected band diagram of hexagonal lattice (**c**) Band diagram analysis of Square lattice (**d**) Projected band diagram of square lattice

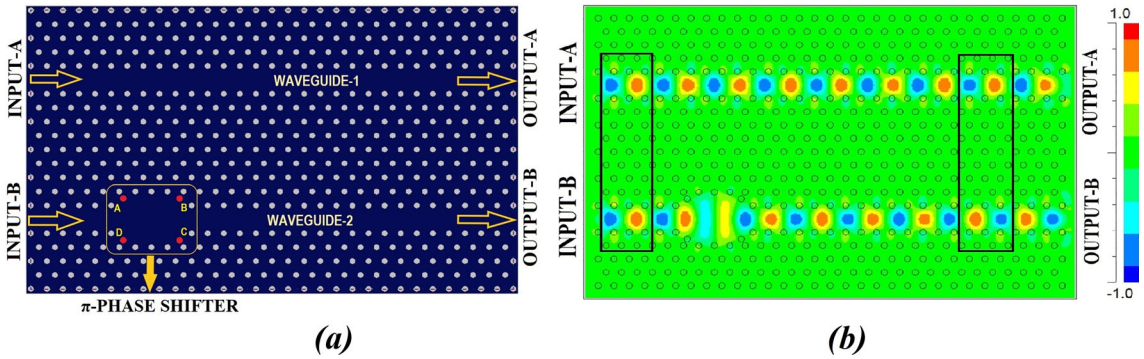

Fig. 2 Schematic design of Π phase shifter of (**a**) Two-dimensional model (**b**) Electric field propagation profile in the device

phase of the optical signal applied to WAVEGUIDE-2. The validation and performance of the proposed phase shifter have been explained in the subsequent subsections.

3.1 Validation and result analysis of Π phase shifter

The proposed π-phase shifter has been validated by implementing an optical XOR gate, which operates on the principle of light beam interference. It is observed that the use of an asymmetric Y-shaped waveguide led to the creation of a π-phase difference, which behaves as an XOR gate. To address this issue, a symmetric Y-shaped waveguide can be utilized for the XOR operation by embedding a π-phase shifter in one of the input waveguides. A Y-shaped structure (two input ports, INPUT-A & INPUT-B and one output port, OUTPUT) has been designed with a footprint of 301 μm^2 on a 2D-PhC platform for this purpose, where two input waveguides (WA-1 and WA-2) and an output waveguide (W5) are present. The input waveguides WG-1 and WG-2 intersect with waveguides WG-3 and WG-4, respectively, by making a 60-degree bend at junctions C1 and C2. Additionally, waveguides WG-3 and WG-4 meet at junction C3 to create output waveguide WG-5, forming a Y-shaped structure as shown in Fig. 3a. The lengths of C1C3 and C2C3 have been chosen to be symmetrical, and the proposed π-phase shifter has been placed in WG-2.

To analyze the functionality of the proposed phase shifter, the FDTD algorithm has been applied. The signals (P_i = input power) with the same phase have been applied to both input waveguides. Upon passing

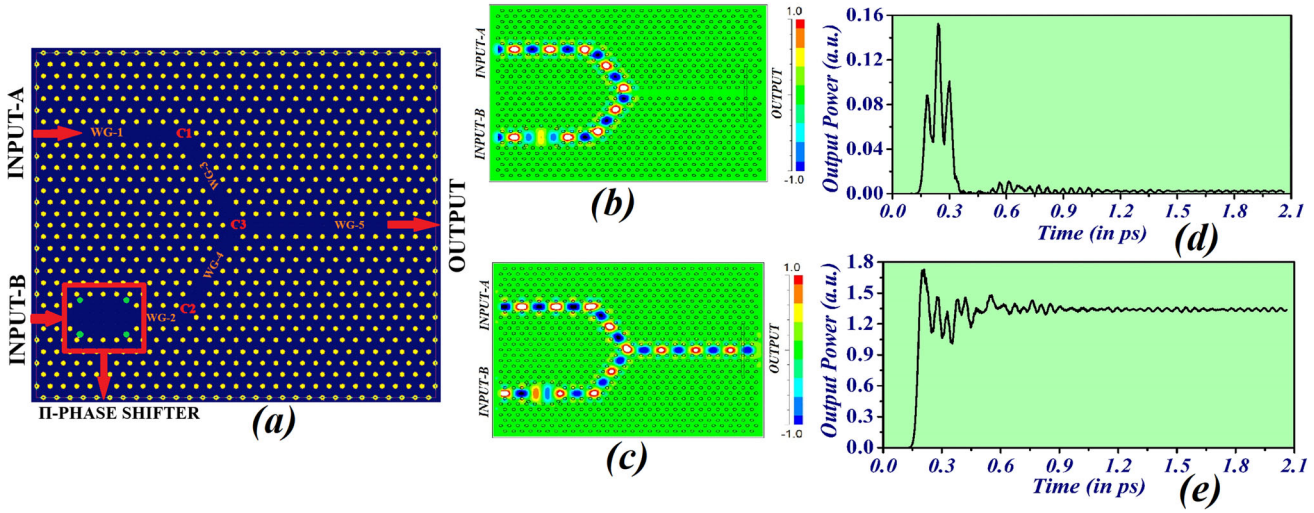

Fig. 3 (**a**) XOR operation in symmetric PhC structure using Π phase shifter. Electric field profile of XOR operation (**b**) when input-A = 0°and input-B = 0° (**c**)when input-A = 0° and input-B = 180°. Time evolving graph of the XOR operation (**d**) when input-A = 0° and input-B = 0° (**e**) when input-A = 0° and input-B = 180°

through the waveguide with the phase shifter, the signal's phase has been observed to be altered by 180 degrees. When both signals meet at the junction (C3), a destructive interference occurs, and no signal (0.001 * P_i) is detected at the output port, as shown in Fig. 3b and 3d. In addition, a signal with a phase of 180-degree was applied to WG-2, while a signal with a phase of 0-degrees has been applied to WG-1. Upon passing through the phase shifter, again, the phase of the signal is observed to be altered by 180-degree. This led to constructive interference at the junction (C3), resulting in a high output power (1.3 * P_i) observed at the output port, as shown in Fig. 3c, e. From the electric field propagation profiles shown in Fig. 3b, c, and the time-evolving graphs shown in Fig. 3d, e, it is completely validated that the proposed Π-phase shifter is capable of altering the signal's phase by 180 degrees. Overall, these validation methods serve to confirm the effectiveness of the design and ensure that it is capable of achieving its intended purpose.

3.2 Operating bandwidth

The performance of the proposed Π-phase shifter has been evaluated across a wavelength range of 1540 nm to 1560 nm, which was simultaneously applied to both INPUT-A and INPUT-B of the optical XOR gate (Fig. 3a). Based on the graph provided in Fig. 4, a maximum output power of approximately 2.5% (0.025 * P_i) has been obtained in the mentioned wavelength range. However, during the XOR operation, almost no output power has been delivered in the wavelength range of 1544 nm to 1556 nm, which correspond to equivalent frequency levels of 194.3THz and 192.8THz, respectively. Therefore, the bandwidth of the proposed phase shifter can be determined as the difference between

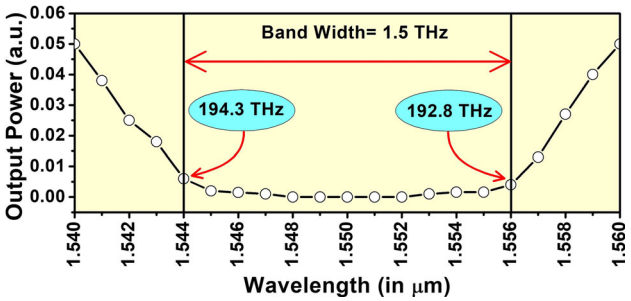

Fig. 4 Band Width of the Π-phase shifter

these two frequencies, which is 1.5THz, as depicted in Fig. 4.

4 Π/2 Phase shifter

The proposed π/2-phase shifter, depicted in Fig. 5a, is designed using a 2D photonic crystal slab. Similar to the π-phase shifter, two straight waveguides, WAVEGUIDE-1 and WAVEGUIDE-2, are created using a line defect to propagate the input signal by removing rods in the Γ-X direction of the PhC. To create the π/2-phase shifter within the waveguide, two rows of rods (four rods in each row) in the Γ-X direction have been removed from a certain portion of the W1 waveguide, and the W3 waveguide is formed. At the corner portion of the W3 waveguide, the radius of the rods, designated as ABCD, is optimized to be 1.2 times the existing radius, and it has been shifted to the Γ-M direction (which is away from the central waveguide) by a distance of Period/2.

Additionally, a new design for a π/2-phase shifter (shown in Fig. 5c) has been created using a rods-in-air

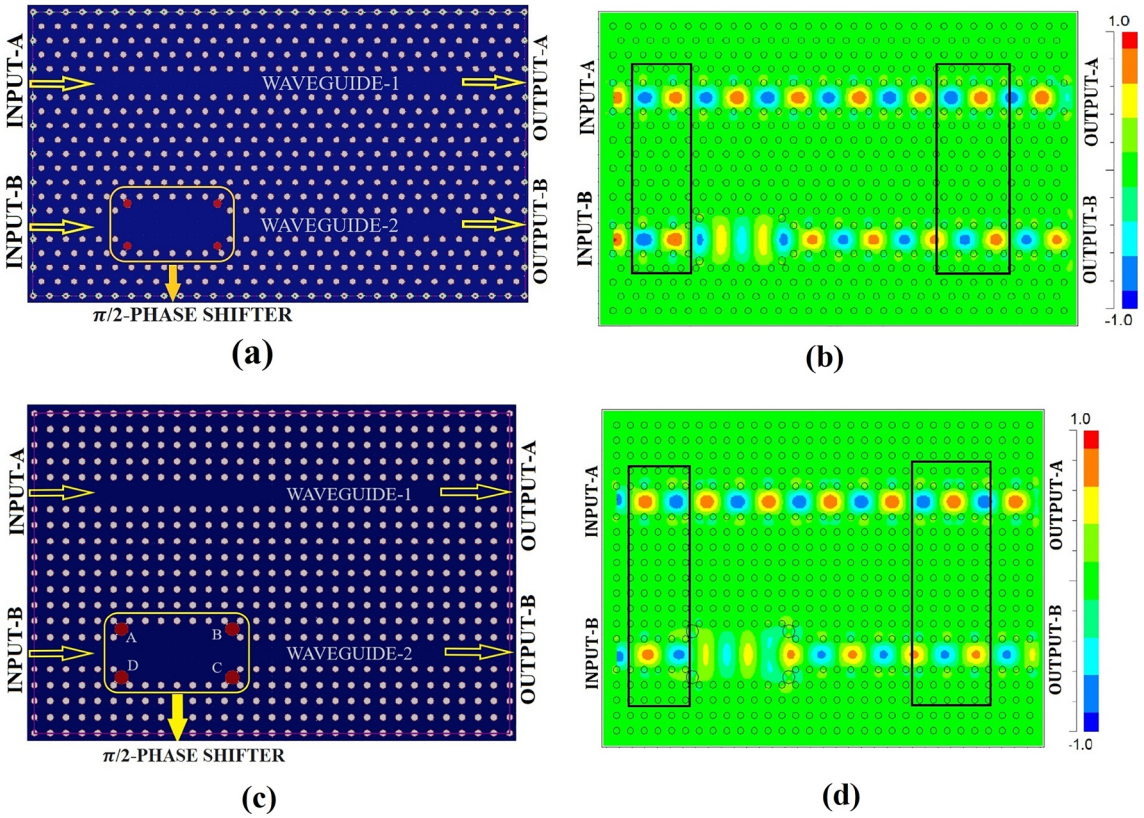

Fig. 5 Schematic design of Π/2 phase shifter of (**a**) Two-dimensional model in triangular lattice (**b**) Electric field propagation of triangular lattice (**c**) Two-dimensional model in square lattice. (**d**) Electric field propagation for square lattice

2D-PhC structure. The rods, with a lattice constant of 540 nm and a radius of 120 nm (0.22 * a, where 'a' represents the lattice constant or period), are placed in a cubic lattice structure in the air background to create the photonic crystal. To create the π/2-phase shifter, two rows of rods (with five rods in each row) have been removed from a specific location in the Γ-X direction in WAVEGUIDE-1 to create the W3 waveguide. Furthermore, the radius of the corner rods (A, B, C & D) of the W3 waveguide has been optimized as doubled, and they have been shifted by a distance of Period/2 in the Γ-M direction away from the central waveguide.

In order to test the functionality of the proposed devices, two identical continuous optical signals have been fed into the input ports of both waveguides of both the devices. The electric field propagation profiles (of both the devices) of the two parallel waveguides have been then obtained using the finite difference time domain (FDTD) algorithm, as shown in Fig. 5b and d. It is apparent from the figures that the electric field propagation profiles of both waveguides are the same from the input ports up to the starting point of the π/2-phase shifters. Once the optical wave (single mode) enters the π/2-phase shifters, it bifurcates into multiple modes and then recombines with each other, ultimately forming a single mode optical wave with a phase change of π/2 when it emerges from the π/2-phase shifters. Additionally, there is a mismatch in the pattern of electric field propagation profile at the trailing end of both waveguides, indicating a shift in the phase of the optical signal applied to WAVEGUIDE-2 for both the π/2-phase shifters. The verification and performance of the proposed phase shifter are explained in the subsequent subsections.

4.1 Validation and result analysis of Π/2 phase shifter

The performance of the proposed Π/2 phase shifter (designed in triangular lattice platform) has been analyzed by designing a Y-shaped structure (with a footprint of 301 μm^2) with two input ports (INPUT-A and INPUT-B) and one output port (OUTPUT) on a 2D-PhC platform where two input waveguides (WA-1 and WA-2) and an output waveguide (W5) are present (refer to Fig. 6a). To verify the functionality of the π/2-phase shifter in the proposed design, a signal (with input power of P_i) with a phase of 0-degree is applied at INPUT-A and a signal (with input power of P_i) with a phase of 90-degree is applied at INPUT-B, where the proposed phase shifter is embedded (refer to Fig. 6b). Upon passing through the waveguide with the phase shifter, both signals meet with each other and underwent destructive interference at junction C3, resulting in no output signal in the output waveguide (as shown in Fig. 6b). Furthermore,

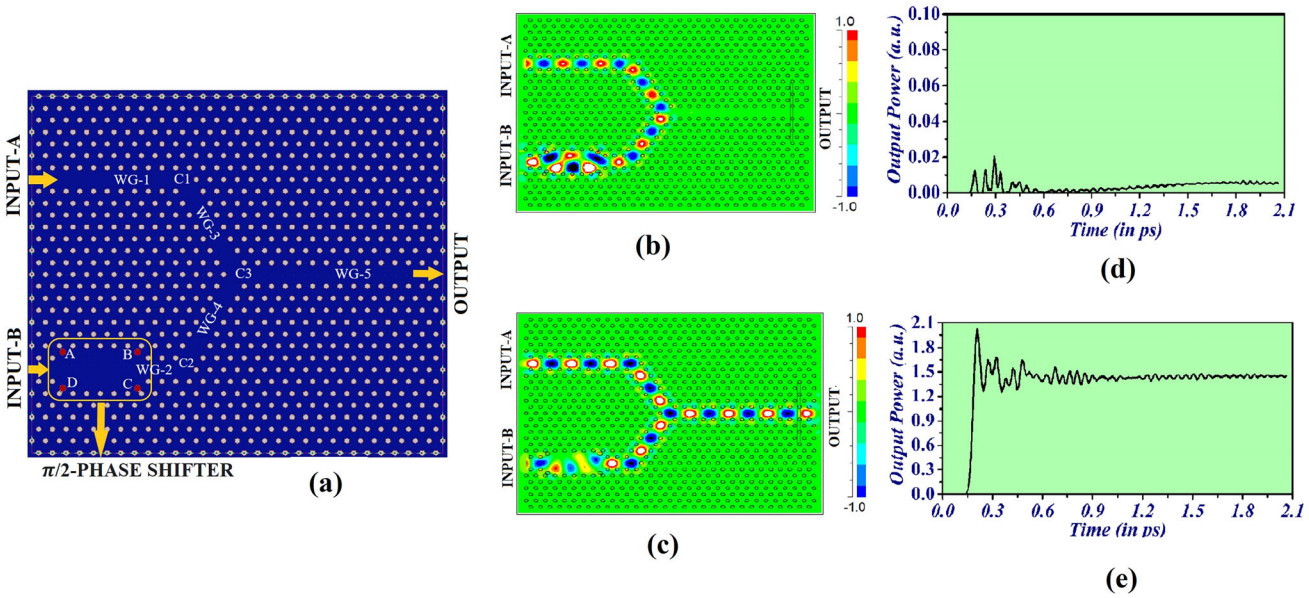

Fig. 6 (**a**) XOR operation in symmetric PhC structure using Π/2 phase shifter. Electric field profile of XOR operation in triangular lattice (**b**) when input –A = 0 degree and input-B = 90degree. (**c**) when input –A = 90 degree and input-B = 0degree. Time evolving graph of the XOR operation in triangular lattice (**d**) when input –A = 0 degree and input B = 90 degree. (**e**) when input –A = 90 degree and input B = 0 degree

Fig. 6c shows that a signal with a phase of 90 degrees is applied to INPUT-A, while a signal with a phase of 0 degrees is applied in INPUT-B. As the signal (applied at INPUT-B) passed through the Π/2 phase shifter and interacts with another input signals (applied at INPUT-A), they underwent constructive interference at junction C3, resulting in a maximum output signal in the output waveguide. Figure 6d and e display the time-evolving graphs for various input conditions. It is evident from the obtained graphs that null power (0.001 * P_i) is achieved at the output when destructive interference occurs, while significant power (more than 1.5 Pi, where Pi represents the input signal power) is obtained when constructive interference occurs. The above-mentioned observations confirm that the proposed Π/2-phase shifter (designed in triangular lattice structure) is capable of altering the signal's phase by 90-degree.

To evaluate the performance of the proposed Π/2 phase shifter (designed on square lattice platform), a Y-shaped like structure (with a footprint of 297 μm^2) with two input ports (INPUT-A and INPUT-B) and one output port (OUTPUT) is designed on a 2D-PhC platform, as shown in Fig. 7a. The structure includes two input waveguides (WA-1 and WA-2) and an output waveguide (W5). To verify the functionality of the phase shifter, a signal with a phase of 0-degree has been applied at INPUT-A, whereas a signal with a phase of 90-degree was applied at INPUT-B, as shown in Fig. 7b. As the signal passes through the phase shifter and meets with another signal at junction C3, they underwent destructive interference at junction C3, resulting in no output signal (0 * P_i) in the output waveguide. Conversely, when a signal with a phase of 90-degree is applied to INPUT-A and a signal with a phase of 0-degree is applied to INPUT-B, the signals underwent constructive interference at junction C3, resulting in a maximum output signal (1.2 * P_i) in the output waveguide, as shown in Fig. 7c. Time-evolving graphs for various input conditions have been presented in Fig. 7d and e, revealing that no signal power is obtained at the output during destructive interference, while substantial power (more than 1.2 Pi, where Pi represents the input signal power) is obtained during constructive interference. Based on the above observations, we can conclude that the proposed Π/2-phase shifter, designed in a square lattice structure, is indeed capable of altering the phase of the signal by 90 degrees.

4.2 Bandwidth

The performance of the π/2 phase shifter has been evaluated in both hexagonal and cubic lattice structures over a wavelength range of 1.540 μm to 1.560 μm, applied simultaneously to both inputs of the Y-shaped structure, as depicted in Figs. 6a and Fig. 7a. Based on the graph provided in Fig. 8, a maximum output power of approximately 2% (0.02 * P_i) has been observed in the wavelength range of 1540 nm to 1560 nm for the hexagonal lattice domain, as shown in Fig. 8a. In the cubic domain, a maximum output power of 2.5% (0.025 * P_i) has been observed in the wavelength range of 1540 nm to 1560 nm, as depicted in Fig. 8b. The XOR operation yielded almost no output power in the wavelength range of 1542 nm to 1557 nm, which corresponds to equivalent frequency levels of 194.5THz and 192.6THz, respectively. Therefore, the bandwidth of the

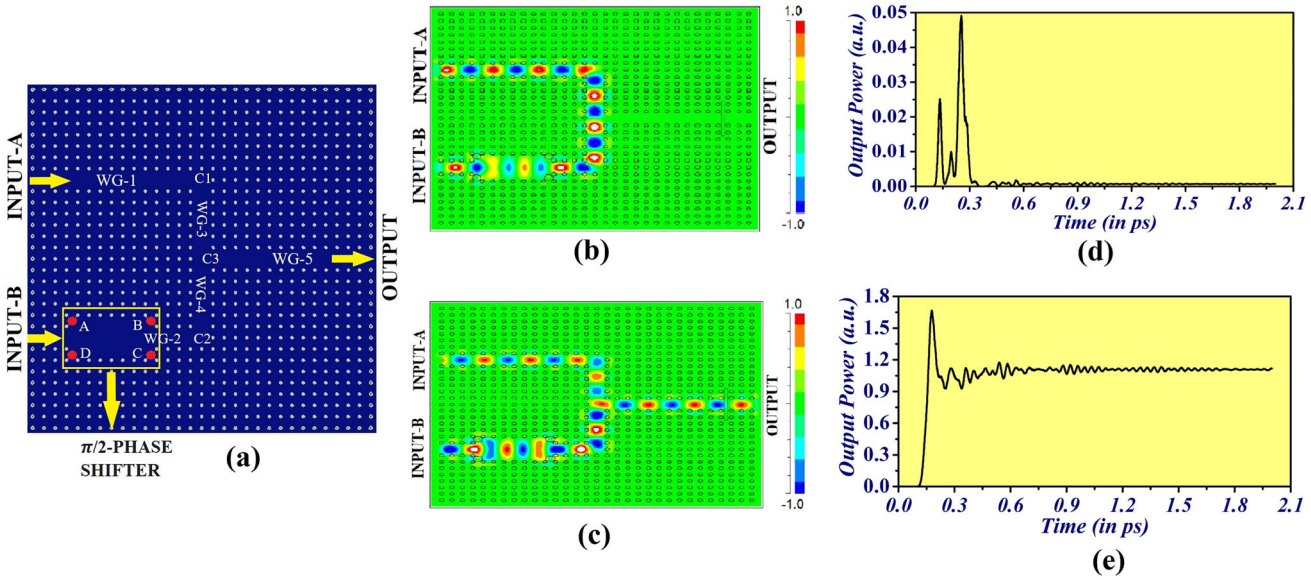

Fig. 7 (**a**) XOR operation in symmetric PhC structure using Π/2 phase shifter. Electric field profile of XOR operation in square lattice (**b**) when input –A = 0 degree and input B = 90 degree. (**c**) when input –A = 90 degree and input B = 0 degree. Time evolving graph of the XOR operation in square lattice. (**d**) when input –A = 0 degree and input B = 90 degree. (**e**) when input –A = 90 degree and input B = 0 degree

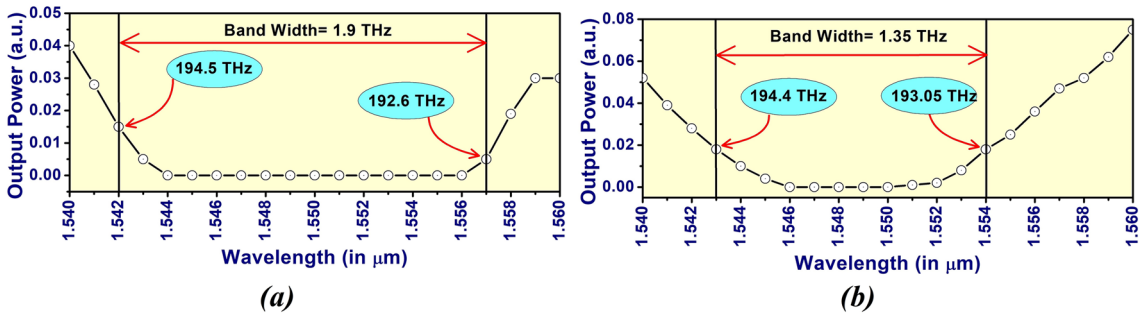

Fig. 8 Band Width of Π/2-phase shifter (**a**) for hexagonal lattice (**b**) for Square lattice

proposed π/2-phase shifter designed on a hexagonal lattice is determined as the difference between these two frequencies, which is 1.9THz, as shown in Fig. 8a. Similarly, the π/2-phase shifter designed on a square lattice delivered almost zero output power in the wavelength range of 1543 nm to 1554 nm, which corresponds to equivalent frequency levels of 194.4THz and 193.05THz, respectively. Hence, the bandwidth is determined as the difference between these two frequency values, which is 1.35THz, as depicted in Fig. 8b.

5 Conclusion

This article proposes a new design for one Π-phase shifter and two Π/2-phase shifters, which are based on a two-dimensional PhC structure. The proposed Π-phase shifter and one Π/2-phase shifter are designed with air-suspended dielectric rods arranged in a triangular lattice, while the other Π/2-phase shifter is designed with a square lattice. These structures require no additional external energy or optical nonlinearity to function as phase shifters. FDTD simulation results demonstrate that the Π-phase shifters can operate within the wavelength range of 1544 nm to 1556 nm, providing a large bandwidth of 1.5 THz. The Π/2-phase shifters provide operating bandwidths of 1.9THz and 1.35THz, respectively. The simplicity of the structural design, absence of external energy, and large operating bandwidth make these proposed phase shifters potential candidates for future-generation photonic integrated circuits.

Acknowledgements Not applicable.

Author contribution

H.M., N.D., M.M.D., S.B., K.G., S.D., M.S. have equally contributed toward designing the devices, simulating the

structures, preparing pictures, graphs and manuscript. All the authors have read and approved the final manuscript.

Funding The authors did not receive fund from any organization for the submitted work.

Data Availability Statement This manuscript has no associated data or the data will not be deposited. [Authors' comment: The data contained in this article are all in the tables and figures in the article, that is, the data are displayed in the form of charts. All data generated or analyzed during this study are included in this published article.]

Declarations

Conflict of interest The authors have no competing interests to declare that are relevant to the content of this article.

Ethical approval We declare that the manuscript entitled "Design and Simulation of Phase Shifter based on Multimode Interference in Photonic Crystal Waveguide" is original, has not been fully or partly published before, and is not currently being considered for publication elsewhere. Moreover, we further confirm that the order of authors listed in the manuscript has been approved by all of us.

Consent to participate Not applicable.

Consent for publication Not applicable.

References

1. M. Mohammadi, M. Soroosh, A. Farmani, S. Ajabi, "Engineered FWHM enhancement in plasmonic nanoresonators for multiplexer/demultiplexer in visible and NIR range" Optik, vol. 274, March 2023, 170583.
2. A. Khajeh, Z. Hamzavi-Zarghani, A. Yahaghi et al., Tunable broadband polarization converters based on coded graphene metasurfaces. Sci. Rep. **11**, 1296 (2021)
3. A. Vahdat, H. Liu, X. Zhao, C. Johnson, The emerging optical data center, Optical Fiber Communication Conference/National Fiber Optic Engineers Conference 2011, paper OTuH2 (2011)
4. Y. Taga, Recent progress of optical thin films in the automobile industry. Appl. Opt. **32**, 5519–5530 (1993)
5. G.L. Cote, R.M. Lec, M.V. Pishko, Emerging biomedical sensing technologies and their applications. IEEE Sens. J. **3**(3), 251–266 (2003). https://doi.org/10.1109/JSEN.2003.814656
6. H. Cheng, Xu. Chunyun, X. Jing, H.-Y. Tam, Design of compact LED free-form optical system for aeronautical illumination. Appl. Opt. **54**, 7632–7639 (2015)
7. K. Goswami, H. Mondal, M. Sen, Optimized design of multiple bends for maximum power transfer in optical waveguide, Optik, vol. **265**, page no. 169448, (2022).
8. K. Goswami, H. Mondal, M. Sen, Optimized design of 60° bend in optical waveguide for efficient power transfer, In: Bera R., Pradhan P.C., Liu CM., Dhar S., Sur S.N. (eds) Advances in Communication, Devices and Networking, Lecture Notes in Electrical Engineering **662**, Springer, (2020).
9. S. Khani, A. Farmani, A. Mir, Reconfigurable and scalable 2,4-and 6-channel plasmonics demultiplexer utilizing symmetrical rectangular resonators containing silver nano-rod defects with FDTD method. Sci. Rep. **11**, 13628 (2021)
10. F. Pakrai, M. Soroosh, J. Ganji, A novel proposal for an all-optical combined half adder/subtractor. Opt. Quant. Electron. **54**, 518 (2022). https://doi.org/10.1007/s11082-022-03898-z
11. M. Mansuri, A. Mir, A. Farmani, A tunable nonlinear plasmonic multiplexer/demultiplexer device based on nanoscale ring resonators. Photon Netw. Commun. **42**, 209–218 (2021). https://doi.org/10.1007/s11107-021-00953-9
12. H.P. Mondal, M. Sen, K. Goswami, Design and analysis of all-optical 1-to-2-line decoder based on linear photonic crystal. IET Optoelectronics (IET) **13**(4), 191–195 (2019)
13. K. Goswami, H. Mondal, M. Sen and A. Sharma., "Design and Analysis of All-Optical Isolator Based on Linear Photonic crystal", Brazilian journal of physics, vol. 52, no. 78, 2022.
14. C. Prakash, M. Sen, H. Mondal, K. Goswami, Design and optimization of a TE pass polarization filter based on a slotted photonic crystal waveguide. Journal of the Optical Society of America B **35**(8), 1791–1798 (2018)
15. H. P. Mondal, S. Chanda, M. Sen and T. Datta, "All-Optical AND Gate based on Silicon Photonic crystal," IEEE International Conference on Microwave and Photonics, Indian School of Mines, Dhanbad, Jharkhand, 2015.
16. J.D. Joannopoulos, S.G. Johnson, J.N. Winn, R.D. Meade, *Photonic Crystals: Molding the Flow of Light*, 2nd edn. (Princeton Univ, Press, 2008)
17. E. Yablonovitch, Inhibited spontaneous emission in solid-state physics and electronics. Phys. Rev. Lett. **58**, 2059–2062 (1987)
18. K. Goswami, H. Mondal, M. Sen, A review on all-optical logic adder: Heading towards next-generation processor. Optics Communications **483**, 126668 (2021)
19. F. Parandin, A. Sheykhian, Design of an all-optical half adder based on photonic crystal ring resonator. Opt. Quant. Electron. **54**, 443 (2022). https://doi.org/10.1007/s11082-022-03810-9
20. M. Abdollahi, F. Parandin, A novel structure for realization of an all-optical, one-bit half-adder based on 2D photonic crystals. J. Comput. Electron. **18**, 1416–1422 (2019). https://doi.org/10.1007/s10825-019-01392-6
21. F. Parandin, R. Kamarian, M. Jomour, A novel design of all optical half-subtractor using a square lattice photonic crystal. Opt. Quant. Electron. **53**, 114 (2021). https://doi.org/10.1007/s11082-021-02772-8
22. F. Parandin, A. Sheykhian, "Design and simulation of a 2 × 1 All-Optical multiplexer based on photonic crystals", Optics & Laser Technology, Vol. 151, page no. 108021, 2022.
23. H.P. Mondal, K. Goswami, M. Sen, C. Prakash, An all-optical ultra-compact 4-channel wavelength de-multiplexer, IEEE International Conference on Microwave and Photonics, Indian School of Mines, Dhanbad, Jharkhand, (2018).

24. D. Gogoi, K. Das, H. P. Mondal, P. Talukdar, K. Hussain, Design of ultra-compact 3-channel wavelength demultiplexer based on photonic crystal, IEEE international conference on automatic control and dynamic optimization technique (ICACDOT-2016), I2IT, Pune, Maharashtra, (2016).
25. H. Mondal, M. Sen, K. Goswami, Design and analysis of a 0.9 Tb/s six-channel WDM filter based on photonic crystal waveguides. J. Opt. Soc. Am. B **36**, 3181–3188 (2019)
26. S. Serajmohammadi, H.A. Banaei, F. Mehdizadeh, A novel proposal for all optical 1-bit comparator using nonlinear PhCRRs. Photon. Nanostruct. Fundam. Appl. **34**, 19–23 (2019)
27. M. Noori, M. Soroosh, H. Baghban, Design of highly efficient polarization beam splitter based on self-collimation on Si platform. J. Mod. Opt. **64**, 491–499 (2017)
28. H. Saghaei, A. Zahedi, R. Karimzadeh, F. Parandin, Line defects on As2Se3 chalcogenide photonic crystals for the design of all optical power splitter and digital logic gates. Superlattices Microstruct. **110**, 133–138 (2017)
29. F. Mehdizadeh, M. Soroosh, and H. A. Banaei, "A novel proposal for optical decoder switch based on photonic crystal ring resonators", Optical Quantum Electronics, vol. 48, no. 20, 2016.
30. F. Mehdizadeh, H. A-Banaei, S. Serajmohammadi, "Design and simulation of all optical decoder based on nonlinear PhCRRs", Optik, Vol: 156, pp. 701–706, 2018.
31. M. J. Maleki, M. Soroosh and A. Mir, "Improving the Performance of 2-To-4 Optical Decoders Based on Photonic Crystal Structures", Crystals, vol. 9, no. 12, 2019.
32. T. Daghooghi, M. Soroosh, K. Ansari-Asl, A low-power all optical decoder based on photonic crystal nonlinear ring resonators. Optik **174**, 400–408 (2018)
33. T. Daghooghi, M. Soroosh, K. Ansari-Asl, Slow light in ultracompact photonic crystal decoder. Appl. Opt. **58**, 2050–2057 (2019)
34. H.P. Mondal, M. Sen, C. Prakash, K. Goswami, and C. Sarma "Impedance matching theory to design all-optical AND gate", IET Optoelectronics (IET), vol-12, issue-4.
35. K. Goswami, H.P. Mondal, P. Das and K. Thakuria "Realization of ultra-compact all-optical logic AND gate based on photonic crystal waveguide", in book Advances in Communication, devices and networking, LNEE Springer Nature, Singapore, ISBN- 978–981–16–2910–5, vol. 776, pp. 61–68.
36. A. Farmani, A. Mir, M. Irannejad, 2D-FDTD simulation of ultra-compact multifunctional logic gates with nonlinear photonic crystal. J. Opt. Soc. Am. B **36**, 811–818 (2019)
37. H. Mondal, K. Goswami, M. Sen, W. R. Khan, "Design and analysis of all-optical logic NOR gate based on linear optics," Optical and Quantum Electronics (2022), vol. 54, no. 272.
38. F. Parandin, N. Mahtabi, Design of an ultra-compact and high-contrast ratio all-optical NOR gate. Opt. Quant. Electron. **53**(12), 1–9 (2021)
39. A. Malik, S. Dwivedi, L. Van Landschoot et al., Ge-on-Si and Ge-on-SOI thermo-optic phase shifters for the mid-infrared. Opt. Express **22**, 28479–28488 (2014)
40. S. Zhu, G.-Q. Lo, Aluminum nitride electro-optic phase shifter for backend integration on silicon. Opt. Express **24**, 12501–12506 (2016)
41. N. Dhingra, J. Song, G. J. Saxena, E. K. Sharma and B. M. A. Rahman, "Design of a Compact Low-Loss Phase Shifter Based on Optical Phase Change Material," in *IEEE Photonics Technology Letters*, vol. 31, no. 21, pp. 1757–1760, 1 Nov.1, 2019, https://doi.org/10.1109/LPT.2019.2946187.